Desalination and Water Treatment
www.deswater.com

doi: 10.5004/dwt.2017.21683

100 (2017) 126–134
December

Synthesis of ureido-functionalized Cr(VI) imprinted polymer: adsorption kinetics and thermodynamics studies

Fang Zhu*, Yanhong Lu, Tengfei Ren, Siying He, Yaqin Gao

College of Environmental Science and Engineering, Taiyuan University of Technology, Taiyuan, Shanxi, 030024, China
Tel. +86 13935188516, Fax +86 3516018786, email: zhufang@tyut.edu.cn (F. Zhu), Tel. +86 15735181327, email: 1359219683@qq.com (Y. Lu), Tel. +86 13935188516, email: 2583843614@qq.com (T. Ren), Tel. +86 18406570822, email: 514889206@qq.com (S. He), Tel. +86 18734821223, 1457680369@qq.com (Y. Gao)

Received 9 January 2017; Accepted 17 November 2017

ABSTRACT

To achieve a fast adsorption and a high adsorption capacity, a new type of Cr(VI) surface ion imprinted polymer (Cr(VI)-IIP) using γ-ureidopropyltrimethoxysilane as a functional monomer was prepared and characterized by scanning electron microscope (SEM) and fourier transform infrared spectroscopy (FTIR). The adsorption capacity of Cr(VI)-IIP was 1.96 times as high as NIP under the optimum conditions: the initial concentration of Cr(VI) ions was 100 mg/L, dosage of Cr(VI)-IIP was 0.01 g, pH value was 2, temperature was 303.15 K. The adsorption process of Cr(VI)-IIP followed pseudo-second-order kinetic model ($R^2 > 0.99$) and Langmuir adsorption isotherm model($R^2 > 0.99$). Results of intraparticle diffusion and external mass transfer models showed that the adsorption process was controlled by liquid film diffusion and intra-particle diffusion model. The adsorption process belonged to the endothermic reaction and could occur spontaneously. Cr(VI)-IIP showed good selectivity and the relative selectivity coefficients were 4.79, 3.44 and 4.50 for Cr(VI)/Cu(II), Cr(VI)/Cd(II) and Cr(VI)/Zn(II), respectively.

Keywords: Cr (VI)-ion surface imprinted polymer; Adsorption; Hexavalent Chromium Ions; Kinetics; Thermodynamics

1. Introduction

In recent years, heavy metals caused serious water contamination because they are toxic and could cause great harm to human and environment. Among these heavy metals, hexavalent chromium (Cr(VI)) is highly toxic and well known as a carcinogen [1], which is the second most abundant inorganic contaminant in groundwater [2]. The Cr(VI) in the environment is mainly from the emission of electroplating, metallurgy, leather processing etc., causing a tremendous threat to environment and human health [3,4]. Therefore, it is necessary to remove Cr(VI) from wastewater. The common chemical treatment methods, such as chemical precipitation method [5], ion-exchange method [6], membrane separation method [7], etc., existing a variety of problems including the secondary pollution, expensive, energy consuming, etc. Adsorption is widely used to remove Cr(VI) ions from wastewater because of its simple operation and high removal rate. However, adsorbents such as chitosan [8], active carbon [9], and carbon nano tubes [10] have the disadvantages of poor selectivity and specificity towards target ions. Therefore, there is an urgent need to develop inexpensive and environmentally friendly adsorbents to Cr(VI) ions in the aqueous solution.

Ion imprinting technique is derived from molecular imprinting technology. Specific recognition sites on the surface of ion imprinted polymers (IIPs) can identify metal ions, so IIPs have good capability to adsorb and detect heavy metal ion in water [11,12]. Because of low cost and specific recognition capability, IIPs have attracted more and more attention. Currently, Cr(VI) ion-imprinted polymers have been synthesized and used to adsorb chromium ions in waste-

*Corresponding author.

water. Bayramoglu et. al. [13] synthesized the Cr(VI)-ion imprinted poly (4-vinyl pyridine-co-2-hydroxyethyl methacrylate) by bulk polymerization to remove Cr^{6+} selectively, the maximum adsorption capacity was 3.31 mmol/g. Pakade et. al. [14] synthesized a novel Cr(VI)-imprinted polymer by copolymerization of quaternised linear copolymer, the optimum stirring time and the optimum dosage of Cr(VI)-imprinted polymer were 120 min and 130 mg. Nastasović et al. [15] prepared poly(GMA-co-EGDMA)-en and poly(GMA-co-EGDMA)-deta using suspension copolymerization technique. The adsorption capacities were 2.11 and 1.48 mmol/g, respectively. However, the above-mentioned polymers have different limitations, such as long adsorption equilibrium time and small adsorption capacity.

Compared with conventional ion imprinting technology, surface ion imprinting technique has the advantages of accessible binding sites, easy mass transfer and fast removal of template ions etc [16,17]. Li et al. [18] prepared Cr(VI)-anion imprinted polymer (IIP-PEI/SiO^2) with high performances using surface imprinting technique. The equilibrium adsorption amount was 100 mg/g, but the selectivity coefficient was only 12.23 for Cr(VI)/PO^{43-}. Liu et al. [19] prepared Cr(III)-imprinted polymer by surface imprinting technique on the support of mesoporous silica for the adsorption Cr (III) and the adsorption capacity was 38.50 mg/g. According to above researcher's literature, the development of new surface ion imprinting polymers with high property is needed in order to remove Cr(VI) ions in the aqueous solution.

The overall objectives of this study was synthesizing a new type of Cr(VI)-ion surface imprinted polymer (Cr(VI)-IIP) with hexavalent chromium ions as the template ions, γ-ureidopropyltrimethoxysilane as the functional monomer, 2,2-azobisisobutyronitrile (AIBN) as the initiator and ethyleneglycol dimethacrylate (EGDMA) as the cross-linking agent via the surface ion imprinting technique. Scanning electron microscope (SEM) and fourier transform infrared spectrometry (FTIR) were adopted to analyzed the characterization of Cr(VI)-IIP. The influences of initial concentration of Cr(VI) ions, pH values, adsorption time and temperatures on the adsorption capacity were studied in detail. In addition, adsorption kinetics and thermodynamics were also investigated to evaluate the adsorption process.

2. Experimental

2.1. Chemicals and instruments

All of chemicals used in the experiments were of analytical reagent grade. Potassium dichromate ($K^2Cr^2O^7$), ethanol, acetone, silica gel (100–200 mesh), γ-ureidopropyltrimethoxysilane, $CuSO_4{\cdot}5H_2O$, $CdCl_2{\cdot}2.5H_2O$, $Zn(NO_3)_2{\cdot}6H_2O$, and sodium hydroxide (NaOH) for pH adjustment were purchased from Sinopharm Chemical Reagent Co., Ltd., China. 2, 2-Azobisisobutyronitrile (AIBN) was obtained from Shanghai Four Hervey Chemical Co., Ltd., China. Ethyleneglycol dimethacrylate (EGDMA) was obtained from ACROS Organics (New Jersey, USA.). Hydrochloric acid (HCl) for pH adjustment was supplied by Tianjin Jin Feng-Chuan Chemical Co., Ltd., China. Double distilled water (DDW) was prepared by Milli-Q advantage purification system (Merck Millipore Ltd., France).

The measurement of Cr(VI) was carried out with a SP-752 UV-visible spectrophotometer (Shanghai Spectrum Instruments Co., Ltd.). The concentrations of Cd(II), Zn(II) and Cu(II) ions were measured by TAS-990 flame atomic adsorption spectrometer (FAAS) (Beijing General Instrument Co., Ltd., China). The measurement of pH values were carried out by a pHS-3C digital pH meter (Shanghai Precision & Scientific Instrument Co., Ltd., China). Fourier transform infrared spectra (FT-IR, 4500 cm^{-1}–500 cm^{-1}) (Bruker, Germany) with KBr pellets was recorded by Bruker Tensor 27 FT-IR spectrometer. JSM-7100F field emission scanning electron microscope (SEM) (Japan Electron Optice Laboratory Co., Ltd., Japan) was employed to analyze the polymer morphology.

2.2. Preparation of Cr (VI)-ion surface imprinted polymer

Silica gel was activated by 3 mol/L hydrochloric acid (HCl). After stirring continuously for 24 h at 323.15 K, the mixture was filtered and washed to neutral pH using distilled water. Then the activated silica gel was dried in a vacuum oven.

0.6177 g $K_2Cr_2O_7$ was added to the system of ethanol – acetone – distilled water (5:3:5, V/V/V) in a flask and was stirred for 1 h at 323.15 K. 2.425 g γ-ureidopropyltrimethoxysilane dissolved in 10.0 mL of methanol, adding into the flask and stirring continuously for 1 h, then 3.0 g of activated silica gel was added. After purification with nitrogen for 15 min, keeping stirring for 8 h. Then 0.115 g AIBN was dissolved in 20.0 mL of ethanol and 3.7 mL of EGDMA and the mixture was added within 8 h. Finally, the product was washed several times with ethanol and water. After drying, the product was eluted with 1 mol/L HCl until Cr(VI) ions were not detected. Then, it was filtered and washed to neutral pH with double distilled water. The prepared product was dried at 323.15 K in a vacuum. Fig. 1 clearly shows the preparation process of Cr(VI)-ion surface imprinted polymer (Cr(VI)-IIP). In order to compare with Cr(VI)-IIP, the corresponding non-imprinted polymer (NIP) was prepared by the same method without adding template ion.

2.3. Adsorption experiments

Batch adsorption experiments were carried out by adding 0.01 g of Cr(VI)-IIP into 50 mL of different initial concentrations of Cr^{6+} solutions for 80 min in different temperatures. Equilibrium adsorption capacity q_e (mg/g) and adsorption amount q_t (mg/g) at time t (min) of Cr^{6+} ions can be obtained according to Eqs. (1) and (2).

$$q_e = \frac{c_i - c_e}{m} \times v \tag{1}$$

$$q_t = \frac{c_i - c_t}{m} \times v \tag{2}$$

where c_t (mg/L) represents the concentrations of metal ions at time t (min), c_i (mg/L) and c_e (mg/L) are the initial and final concentration of heavy metal ions in solution, v (L) is the volume of solution and m (g) is the weight of Cr(VI)-IIP and NIP.

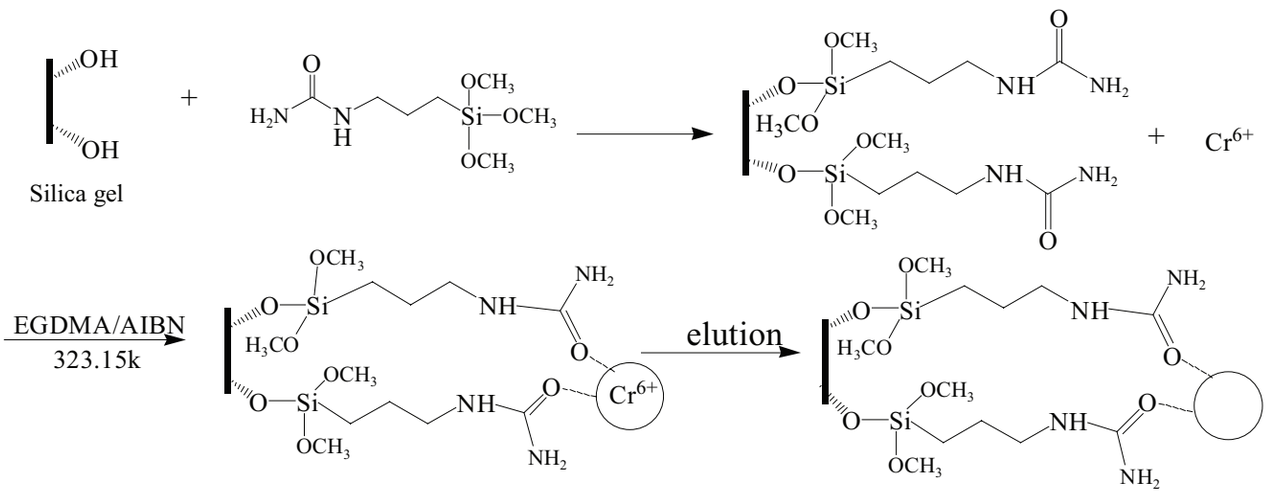

Fig. 1. Synthesis route of Cr(VI) ion imprinted polymer.

3. Results and discussion

3.1. Surface morphology of Cr(VI)-IIP

The surface morphology was analyzed by SEM with a scanning voltage of 10 kV and is shown in Fig. 2. The surface of Cr(VI)-IIP have irregular holes which belonged to active sites after elution. Cr(VI)-IIP with the unique porous structure has larger surface area that would be benefit to the adsorption process.

3.2. FTIR spectra of Cr(VI)-IIP

Cr(VI)-IIP and NIP were characterized by FTIR spectroscopy. The FTIR spectra showed that both Cr(VI)-IIP and NIP had a similar backbone, as shown in Fig. 3. A peak at 1640cm^{-1}~1650 cm^{-1} represents the vibration of –CONH^2, while an intense and broad band at 1100 cm^{-1} can be considered to the stretching vibrations of Si-O-C of Cr(VI)-IIP. The bands at 804 cm^{-1} and 468 cm^{-1} represent O-Si-O and Si-O of silanol groups. Compared with Cr(VI)-IIP, the characteristic peaks of NIP were changed slightly in intensity. Results suggested that the monomer have successfully reacted with silica gel, hence the synthesis of Cr(VI)-IIP is feasible.

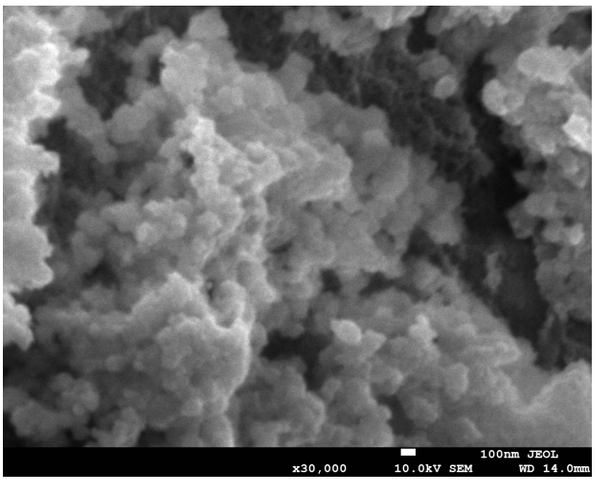

Fig. 2. SEM image of Cr(VI)-IIP.

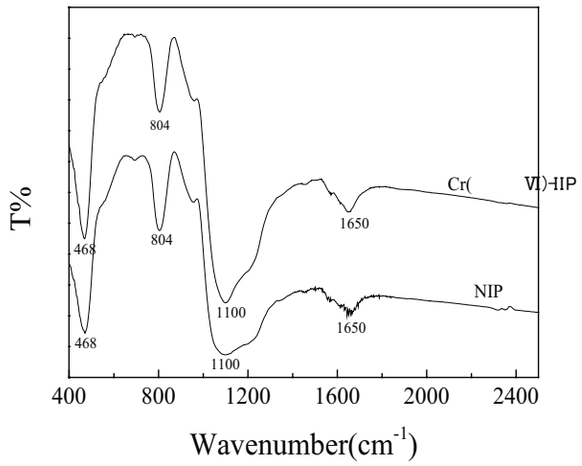

Fig. 3. FTIR curves of Cr (VI)-IIP and NIP.

3.2. Adsorption effect of Cr(VI)-IIP towards Cr(VI) ions

3.2.1. Effect of initial concentration of Cr(VI) ions in the aqueous solution on the adsorption

Fig. 4 displays the effect of different initial concentrations of Cr(VI) ions on the adsorption capacity of Cr(VI)-IIP and NIP clearly. At 303.15 K, the adsorption experiments were carried out in the initial concentration of Cr(VI) ranged from 10 to 200 mg/L at pH = 2.0. As shown in Fig. 4, the adsorption capacity of Cr(VI)-IIP increased from 15.2 mg/g to 41.5 mg/g when the initial concentration of Cr(VI) was increased from 10 mg/L to 100 mg/L. However the adsorption capacity of NIP only increased from 9.1 mg/g to 21.2 mg/g. The adsorp-

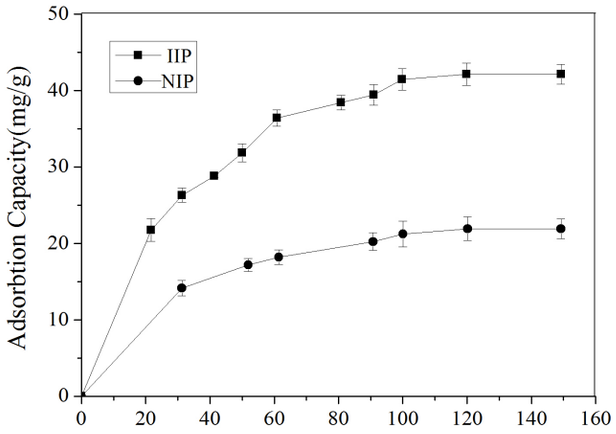

Fig. 4. Effect of Cr (VI) initial concentration on the adsorption capacity of Cr (VI)-IIP and NIP.

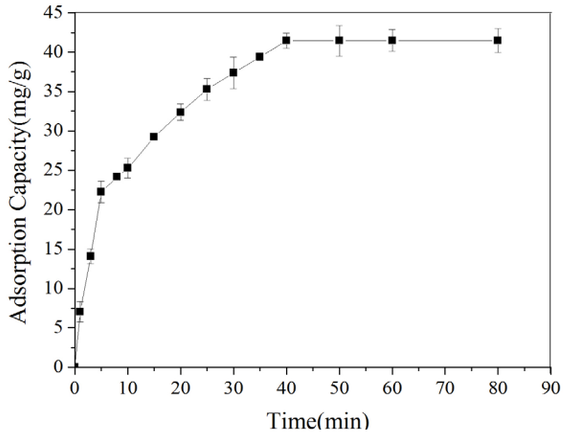

Fig. 5. Effect of adsorption time on the adsorption capacity of Cr (VI)-IIP.

tion capacity of Cr(VI)-IIP and NIP reached saturation when the initial concentration of Cr(VI) ions achieved 100 mg/L, due to the imprinted sites of Cr(VI)-IIP were occupied gradually and finally reached saturation as the concentration of Cr(VI) ions in the solution increased. Thus, when the value of concentration of Cr (VI) ions in the solution was greater than 100 mg/L, the amount of adsorption was not significantly changed. It can be seen from Fig. 4 that the adsorption capacity of Cr(VI)-IIP was twice as high as NIP. It was probably due to the imprinted sites on the Cr(VI)-IIP, whose shape and size match with Cr(VI) ions, leading to the increase of the adsorption capacity. Thus, the optimal concentration of Cr (VI) ions used in subsequent experiments was 100 mg/L.

3.2.2. Effect of adsorption time on the adsorption capacity

Fig. 5 shows the adsorption capacity increased as the adsorption time increased. As shown in Fig. 5, the adsorption process can be divided into three stages. The first stage belonged to linear growth phase: the adsorption capacity increased rapidly from 0 to 22.3 mg/g within 5 min. The second stage was the slow growth phase: the adsorption amount increased by 19.2 mg/g within 35 min. The final stage was the stage of saturation: the adsorption capacity did not change significantly after 40 min in this stage. It can be concluded that the entire process was fast and the adsorption equilibrium achieved within 40 min because there were many imprinted sites on the prepared Cr(VI)-IIP, thus Cr(VI) ions could bind with the imprinted cavities quickly.

3.2.3. Effect of pH on the adsorption

Cr(VI) exists in various forms at different pH values, such as $Cr_2O_7^{2-}$, $HCrO_4^-$, CrO_4^{2-}, H_2CrO_4. According to the literature [20], H_2CrO_4 is the main form in the solution when the pH value is less than 2.0; when pH value is 7.0 or more than 7.0, Cr(VI) is mainly in the form of CrO_4^{2-}; $HCrO_4^-$ and $Cr_2O_7^{2-}$ both exist at pH 2.0–6.0 and the balance expressions are listed below.

$$HCrO_4^- \leftrightarrow CrO_4^{2-} + H^+ \quad (3)$$

$$H_2CrO_4^- \leftrightarrow HCrO_4^- + H^+ \quad (4)$$

$$Cr_2O_7^{2-} + H_2O \leftrightarrow 2HCrO_4^- \quad (5)$$

As one of most important factors affecting the adsorption capacity, the effect of pH value on the adsorption capacity was also studied in this work. The results shown in Fig. 6 indicate that the adsorption capacity of Cr(VI)-IIP for Cr(VI) ions decreased with the pH value increased. The adsorption capacity of Cr(VI)-IIP was achieved 41.5 mg/g at pH 2.0. However, the adsorption capacity decreased sharply to 20.2 mg/g with pH value increased from 2.0 to 4.0. It is probably due to that in acid environment, the ability of $-NH_2$ protonation was promoted with the decreasing of pH value, $Cr_2O_7^{2-}$ and $HCrO_4^-$ predominated when pH value was in the range from 2.0 to 6.0, according to Eqs. (4)–(5). Thus there was a strong adsorption for chromium ions.

3.2.4. Effect of temperature on the adsorption

Temperature is another important factor affecting the adsorption capacity. As shown in Fig. 7, the adsorption capacity increased from 31.4 mg/g to 41.5 mg/g when the temperature rose from 293.15 K to 303.15 K. Results showed that the adsorption rate was accelerated as the temperature increased, leading to the increase of adsorption capacity. However the adsorption capacity rapidly decreased to 24.3 mg/g under the temperature of 313.15 K. In short, the effect of temperature on the adsorption capacity is significant. 303.15 K was selected as the optimum temperature in this experiment.

3.3. Adsorption kinetics of Cr(VI)*-IIP*

The common means of characterizing the adsorption rate is the adsorption kinetics [21]. Pseudo-first-order and pseudo-second-order kinetic models were used to fit the experimental data to calculate the adsorption rate constants.

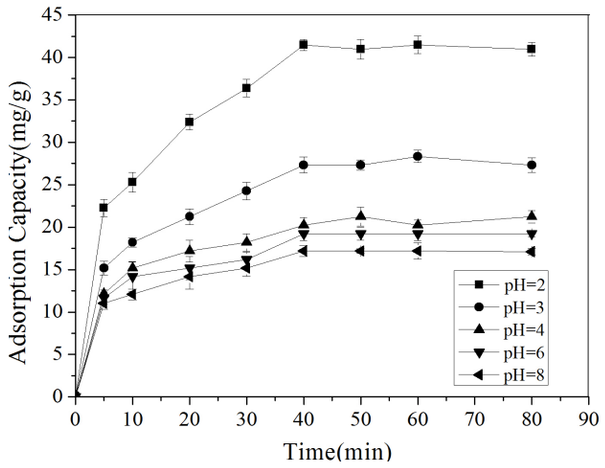

Fig. 6. Effect of pH values on the adsorption capacity of Cr (VI)-IIP.

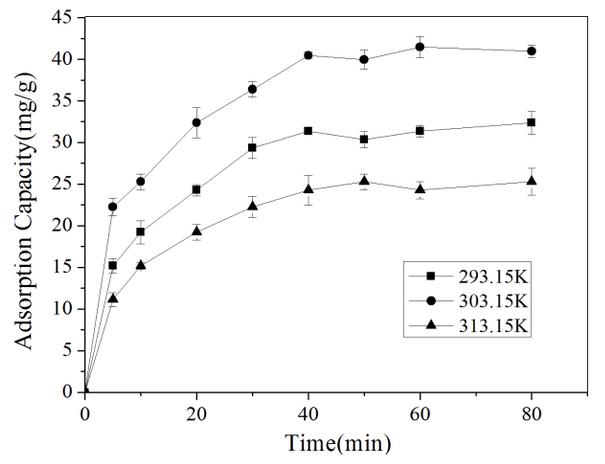

Fig.7. Effect of temperature on the adsorption capacity of Cr (VI)-IIP.

Based on the adsorption of solution from a solid-liquid system, one of commonly used model is Lager gren's equation for pseudo-first order kinetic [22], which can be expressed by Eq. (6):

$$\ln(q_e - q_t) = \ln(q_{1cal}) - k_1 t \tag{6}$$

where q_e (mg/g) and q_t (mg/g) represent the experimentally calculated capacity at equilibrium and at time t (min) respectively; q_{1cal} (mg/g) is the calculated adsorption amount according to the pseudo-first-order equation and k_1 (min^{-1}) is the rate constant of pseudo-first-order adsorption.

The pseudo-second order equation can be written as follows [23]:

$$\frac{t}{q_t} = \frac{1}{k_2 (q_{2cal})^2} + \frac{t}{q_{2cal}} \tag{7}$$

where k_2 ($g \cdot g^{-1}\ min^{-1}$) represents the rate constant of pseudo-second order kinetic model and q_{2cal} (mg/g) is the calculated adsorption amount according to the pseudo-second-order equation, while q_t carries the same meanings as previously defined.

The optimal kinetic model need to be chosen according to the calculated adsorption amount (q_{cal}) and the linear correlation coefficient (R^2). The linear fit of the pseudo-first-order and pseudo-second-order kinetics are shown in Fig. 8. Corresponding linear regression correlation coefficient (R^2), the rate constant (k), the calculated adsorption amount (q_{cal}) and experimentally adsorption capacity (q_e) are listed in Table 1.

On one hand, compared the Fig. 8(a) with 8(b), it can be clearly seen that all the points on Fig. 8(b) are distributed uniformly on both sides of the lines. In addition, the distribution of R^{12} value (0.77964~0.95664) are scattered and are relatively small at different pH values, while the values of R^{22} are greater than 0.99. Results indicated that Cr(VI) adsorption with Cr(VI)-IIP at five different pH values followed the pseudo-second-order, not the pseudo-first-order kinetic model.

On the other hand, the calculated adsorption amount q_{1cal} from the pseudo-first-order kinetic model is significantly lower than the experimental values at five different pH values. However the calculated values q_{2cal} using the pseudo-second-order equation are very close to the experimental ones. Compared with the adsorption capacity at other pH values, the difference between the calculated value q_{2cal} (43.20 mg/g) and the experimental value (41.56 mg/g) is the biggest under pH = 2; the difference is only 1.64 mg/g from the experimental one. It can be further concluded from these results that the pseudo-second-order kinetic can better describe the Cr(VI) adsorption onto Cr(VI)-IIP, suggesting that the adsorption was mainly chemisorption as a rate controlling step [24].

Using the pseudo-first-order and pseudo-second-order kinetics to describe the diffusion mechanism is short of accurateness, the adsorption mechanism was further investigated according to intra particle diffusion and external mass transfer. Intra particle diffusion equation and liquid film diffusion equation are given as follows respectively:

$$q_t = k_{id} t^{1/2} + c \tag{8}$$

$$\ln(1 - F) = -k_f t \tag{9}$$

where k^{id} ($mg\ g^{-1}\ min^{0.5}$) represents the rate constant of intra-particle diffusion model, which can be calculated from the slope of the plot of q_t vs. $t^{1/2}$. $F(q_t/q_e)$ is the fractional attainment of equilibrium, and k_f *(cm/s)* is the rate constant of film diffusion model calculated from the plot of *ln(1–F)* vs. *t*.

The linear plot of intra particle diffusion model for Cr(VI) adsorption onto Cr(VI)-IIP at five different pH values is shown in Fig. 9. The parameters of intra particle diffusion and external mass transfer are shown in Table 2.

As is shown in Table 2, the intercepts of plot of q_t vs. $t^{1/2}$ is not zero, indicating that the adsorption process was multi-step limited to control the adsorption rate. However, the plot of *ln(1–F)* vs. *t* did not go through the origin, revealing that the adsorption of Cr(VI) using Cr(VI)-IIP was controlled by intra particle diffusion model.

As what can be seen clearly from Fig. 9, the Cr(VI) adsorption onto Cr(VI)-IIP at different pH values were divided into three stages. The first stage, namely fast adsorption process, was occurred in the initial 10 min. The second stage, namely gradual adsorption process from 10 to 40

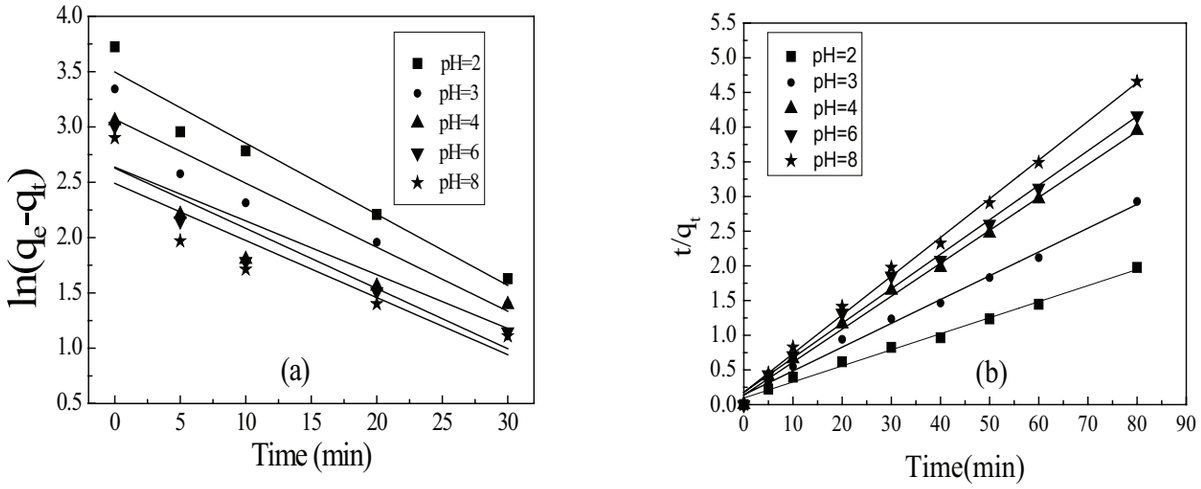

Fig. 8. Pseudo-first-order (a) and Pseudo-second-order (b) kinetics of Cr(VI) adsorption onto Cr(VI)-IIP at five different pH values.

Table 1
Pseudo-first-order and pseudo-second-order rate constants for Cr (VI) adsorption onto Cr (VI)-IIP at different pH values

pH	q_e (mg/g)	Pseudo-first-order model			Pseudo-second-order model		
		R_1^2	k_1 (min^{-1})	q_{1cal} (mg/g)	R_2^2	k_2 (g/mg min)	q_{2cal} (mg/g)
2	41.56	0.9566	0.0643	32.99	0.99226	5.63×10^{-3}	43.20
3	27.32	0.9264	0.0578	21.55	0.99233	8.32×10^{-3}	29.14
4	20.23	0.7796	0.0486	13.97	0.99684	1.65×10^{-2}	21.05
6	19.22	0.8513	0.0544	13.84	0.99309	1.40×10^{-2}	20.10
8	17.20	0.8202	0.0516	12.06	0.99553	1.77×10^{-2}	17.92

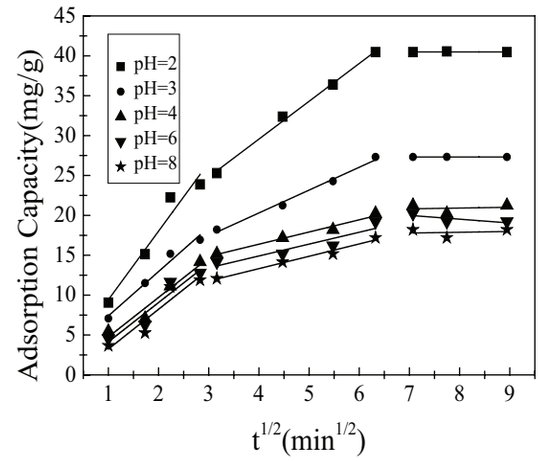

Fig. 9. Intra particle diffusion model for Cr (VI) adsorption onto Cr (VI)-IIP at five different pH values.

min, was controlled by liquid film diffusion and intra-particle diffusion model. The third stage, namely adsorption equilibrium process, was occurred after 40 min where the two diffusion models started to slow down. In addition, it was observed that the values of c_1, c_2 and c_3 for three stages increased as the adsorption time increased, indicating that the liquid film diffusion mechanism became more and more significant with increasing adsorption time.

3.4. *Adsorption isotherms of* Cr(VI)*-IIP and NIP*

The adsorption experiments were carried out under the different initial concentrations of Cr(VI) with 0.01 g Cr(VI)-IIP or NIP for 60 min at pH = 2. Langmuir isotherm model and Freundlich isotherm model were adopted to assess the adsorption performance of Cr(VI)-IIP. Isotherm equations [25] are shown as follows:

$$\frac{c_e}{q_e} = \frac{1}{q_m k} + \frac{c_e}{q_m} \tag{10}$$

where c_e (mg/L) and q_e (mg/g) are the final concentration and the adsorption capacity of Cr(VI), respectively; q_m (mg/g) defines the maximum adsorption capacity which is the slope of the straight line c_e/q_e vs. c_e; k (L/mg) represents the constant of Langmuir model.

$$\ln q_e = \ln k_f + \frac{\ln c_e}{n} \tag{11}$$

where k_f (mg/g) is Freundlich constant calculated from the intercept of the line lnc_e vs. lnq_e, indicating the adsorption

Table 2
The parameters of intra particle diffusion and external mass transfer for Cr (VI) adsorption onto Cr (VI)-IIP

pH	Intra-particle diffusion model						Liquid film model	
	k_{id1}	k_{id2}	k_{id3}	c_1	c_2	c_3	$k_f \times 10^{-3}$	Intercepts
2	8.5934	4.7418	−0.0022	0.8303	10.5898	40.5084	6.02	0.6146
3	5.5590	2.8644	−0.0011	1.8387	8.8450	27.3288	6.13	0.6395
4	4.9510	1.5299	0.0981	−0.1920	10.2652	20.1318	5.50	0.6973
6	4.9249	1.4882	−0.4774	0.7812	8.9557	23.3405	5.37	0.6802
8	4.9890	1.5490	0.0981	−1.7537	7.1253	17.0967	5.70	0.6856

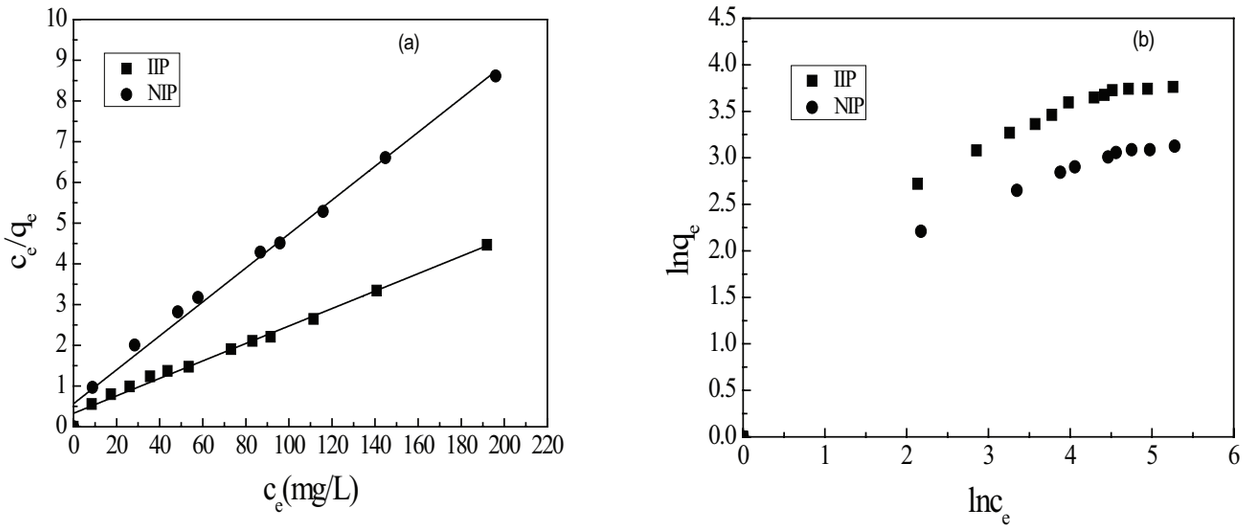

Fig. 10. Linear fit of Langmuir (a) and Freundlich (b) isotherm model for Cr (VI) adsorption onto Cr (VI)-IIP and NIP.

Table 3
Isotherm parameters for Cr (VI) adsorption onto Cr (VI)-IIP and NIP

Adsorbents	q_e (mg/g)	Langmuir model			Freundlich model		
		R^2	q_m	k	R^2	$1/n$	k_f
Cr(VI)-IIP	41.56	0.9900	46.64	0.06499	0.8662	0.6718	2.11
NIP	21.23	0.9914	24.00	0.07378	0.9066	0.5704	1.58

amount; n represents also Freundlich constant obtained from the slope the line lnc_e vs. lnq_e, which is a symbol of the adsorption intensity named the surface heterogeneity index.

The linear fit of Langmuir and Freundlich isotherm model for Cr(VI) adsorption onto Cr(VI)-IIP and NIP is shown in Fig. 10. The isotherm parameters, including corresponding linear regression correlation coefficient and adsorption constants of Langmuir and Freundlich model are summarized in Table 3. As what can be seen from the comparison between Fig. 10a and 10b, all points in Fig. 10a are evenly distributed on both sides of two lines, however all the points in Fig. 10b are centralized. When the correlation coefficient R^2 was used as the criterion to evaluate the goodness of the model with the experimental data, the values of R^2 obtained from the Langmuir model were 0.9900 and 0.9914 for Cr(VI) adsorption using Cr(VI)-IIP and NIP, respectively, while the R^2 values of Freundlich model were 0.8662 and 0.9066 respectively. Langmuir model could describe the adsorption of Cr(VI) onto Cr(VI)-IIP and NIP well. In addition, the values of q_m calculated by the Langmuir model for Cr(VI)-IIP and NIP were 46.64 mg/g and 24.00 mg/g respectively, which were relatively close to the experimental adsorption capacity (Cr(VI)-IIP and NIP are 41.56 mg/g and 21.23 mg/g). Thus the adsorption process of Cr(VI) onto Cr(VI)-IIP and NIP was more similar to the Langmuir adsorption model than Freundlich adsorption model. Furthermore, the constants of Freundlich adsorption model were 0.6718 and 0.5704 for Cr(VI)-IIP and NIP, indicating that the adsorption process of Cr(VI) onto

Cr(VI)-IIP and NIP was based on a typical mono-molecular layer adsorption process.

3.5. Thermodynamic studies

In order to determine the spontaneity of adsorption process, both energy and entropy factors should be considered. Hence, 0.01 g of Cr(VI)-IIP was added into 50 mL 100 mg/L Cr^{6+} solution at different temperatures at pH = 2. The thermodynamic parameters of the adsorption process were calculated according to Eqs. (12)–(14):

$$\Delta G^0 = -RT\ln k_c \tag{12}$$

$$\Delta S^0 = \frac{\Delta H^0 - \Delta G^0}{T} \tag{13}$$

$$\ln k_c = -\frac{\Delta H^0}{RT} + c \tag{14}$$

where ΔG^0, ΔH^0, ΔS^0 represents change in standard free energy, change in standard enthalpy and change in standard entropy, respectively. k_c (mL/g, q_e/c_e) and R (8.314 J·mol^{-1}·K^{-1}) are equilibrium constant and the universal gas constant, respectively.

The calculated thermodynamic parameters are listed in Table 4. As is shown in Table 4, all the values of $\Delta G°$ are less than 0 at different temperatures, suggesting that the adsorption process of Cr(VI) ions on the Cr(VI)-IIP was spontaneous. Meanwhile, the absolute value of $\Delta G°$ at 303.15 K is maximum, illustrating that 303.15 K is the optimum adsorption temperature. A positive value of $\Delta H°$ suggested that the adsorption process belonged to endothermic reaction, indicating that elevating the temperature is beneficial to the increase of adsorption capacity. But the value of $\Delta H°$ is more than 5 kJ·mol^{-1}, revealing that the effect of temperature on the adsorption process was more significant. It is consistent with above results. $\Delta S° > 0$, that is, the entropy was increased in the adsorption process, suggesting that the adsorption of Cr(VI) ions onto Cr(VI)-IIP was a randomness increasing process at solid-liquid interface [26]. The solvent desorbed from Cr(VI)-IIP first, then the solute adsorbed on the Cr(VI)-IIP. The entropy was increased in the desorption process and the entropy was decreased in the adsorption process. The change of entropy in desorption was higher than adsorption, so that $\Delta S°$ was positive. When a Cd(II) ion was adsorbed on the Cr(VI)-IIP, a water molecule would be desorbed and the change of entropy caused by water molecule was higher than Cd(II) ion.

3.6. Selective studies

In order to verify the specificity of Cr(VI)-IIP for Cr(VI) adsorption, Cu(II), Cd(II) and Zn(II) were selected as the competitive ions and mixed with Cr (VI) ions to form the binary mixed solutions respectively. The concentration of Cr(VI), Cu(II), Cd(II) and Zn(II) in the solution were all 100 mg/L. 0.01 g of Cr(VI)-IIP or NIP was added into 50 mL binary mixture solutions at pH = 2 for 40 min. The concentration of Cr^{6+} and competitive ions (Cu(II), Cd(II) and Zn(II)) in the solution were detected by UV-Vis spectrophotometer and FAAS, respectively. The distribution coefficient k_d (mL/g), selectivity coefficient k, and the relative selectivity coefficient k' were calculated according to the formulas (13)–(15) and the results are listed in Table 5.

Table 4
Thermodynamic parameters calculated for the adsorption of Cr (VI) ions on the Cr (VI)-IIP

Temperature/K	lnK^c	ΔG^0/ kJ·mol^{-1}	ΔH^0/ kJ·mol^{-1}	ΔS^0/ J·mol^{-1}
293.15	5.57	–13.57		74.87
303.15	6.11	–15.39	8.38	78.41
313.15	5.78	–15.03		74.78

Table 5
Selectivity coefficient for Cr (VI) adsorption onto Cr (VI)-IIP and NIP

Metal ions	NIP		Cr (VI)-IIP		
	K_d (mL/g)	k	k_d (mL/g)	k	k'
Cr(VI)/	159.39	0.48	498.27	2.31	4.79
Cu(II)	331.02		215.91		
Cr(VI)/	167.18	0.71	476.16	2.46	3.44
Cd(II)	234.24		193.69		
Cr(VI)/	190.06		479.34		
Zn(II)	221.82	0.86	124.39	3.85	4.50

$$k_d = \frac{c_i - c_e}{c_e} \times \frac{v}{m} \tag{15}$$

$$k = \frac{k_{d(Cr(VI))}}{k_{d(M(II))}} \tag{16}$$

$$k' = \frac{k_{(IIP)}}{k_{(NIP)}} \tag{17}$$

where m represents competitive ions, other terms comprising the same meanings have been explained in the foregoing equation.

From Table 5, the selectivity coefficients k were 4.79, 3.44 and 4.50 for Cr(VI)/Cu(II), Cr(VI)/Cd(II) and Cr(VI)/Zn(II), respectively, while the selectivity coefficients k of NIP were only 0.48, 0.71 and 0.86 respectively. It could be concluded that Cr(VI)-IIP can selectively adsorb Cr(VI) when competitive ions coexist in the system, compared with NIP. In addition, the relative selectivity coefficient k' is an indicator to illustrate the affinity of Cr(VI)-IIP. The values of k' for Cr(VI)/Cu(II), Cr(VI)/Cd (II) and Cr(VI)/Zn(II) were found to be 4.79, 3.44 and 4.50, suggesting that the selectivity of Cr(VI)-IIP towards the Cr(VI) ions were 4.79, 3.44 and 4.50 times greater than Cu(II), Cd(II) and Zn(II), respectively.

4. Conclusions

A novel chromium ion imprinted polymer was synthesized for the removal of Cr^{6+} from the aqueous solution, using Cr(VI) as template ion, γ-aureidopropyltrimethox-

ysilane as the functional monomer, 2, 2-zobisisobutyronitrile (AIBN) as initiator and ethyleneglycol dimethacrylate (EGDMA) as cross-linking agent via surface ion imprinting technique. The Cr(VI)-IIP and NIP was characterized by SEM and FTIR. It was found that the optimum adsorption conditions for Cr(VI)-IIP were pH 2.0 at 303.15 K for 40 min. The adsorption capacity of Cr(VI)-IIP were twice higher than NIP at the initial Cr(VI) concentration of 100.0 mg/L under the optimum conditions. The pseudo-second-order kinetic model ($R^2 > 0.99$) and Langmuir adsorption isotherm model ($R^2 > 0.99$) was more suitable to describe the Cr(VI) adsorption onto Cr(VI)-IIP. Thermodynamic studies showed that the adsorption process of Cr^{6+} onto Cr(VI)-IIP belonged to endothermic reaction and could occur spontaneously. Selectivity experiments suggested Cr(VI)-IIP can selectively adsorb Cr(VI) in the presence of other interfering ions and the relative selectivity coefficients were 4.79, 3.44 and 4.50 for Cr(VI)/Cu(II), Cr(VI)/Cd(II) and Cr(VI)/Zn(II), respectively. In conclusion, the Cr(VI)-IIP can absorb Cr^{6+} fast and selectively from aqueous solution.

Acknowledgments

This work was sponsored by the National Natural Science Foundation of China (Project No.21276174) and Natural Science Foundation of Shanxi province (Project No.2013011040-1).

References

[1] B. Dhal, H.N. Thatoi, N.N. Das, B.D. Pandey, Chemical and microbial remediation of hexavalent chromium from contaminated soil and mining/metallurgical solid waste: A review, J. Hazard. Mater., 250–251 (2013) 272–291.
[2] A. Kara, E. Demirbel, N. Tekin, B. Osman, N. Beşirli, Magnetic vinylphenyl boronic acid microparticles for Cr(VI) adsorption: kinetic, isotherm and thermodynamic studies, J. Hazard. Mater., 286 (2015) 612–623.
[3] B. Leśniewska, B.G. Żyłkiewicz, A.Z. Wilczewska, Separation and preconcentration of trace amounts of Cr(III) ions on ion imprinted polymer for atomic absorption determinations in surface water and sewage samples, Microchem. J., 105 (2012) 88–93.
[4] J. Kotaś, Z. Stasicka, Chromium occurrence in the environment and methods of its speciation, Environ. Pollut., 107 (2000) 263–283.
[5] A.J. Jafari, S. Golbaz, R.R. Kalantary, Treatment of hexavalent chromium by using a combined Fenton and chemical precipitation process, J. Water Reuse Desal., 3 (2013) 373–380.
[6] H. Mihçiokur, ìbrahim Peker, Batch study and kinetics of hexavalent chromium removal from aqueous solutions by anion exchange resin (Dowex 21 KCl), Desal. Water Treat., 51 (2013) 2116–2120.
[7] P. Shah, C.N. Murthy, Studies on the porosity control of MWCNT/polysulfone composite membrane and its effect on metal removal, J. Membr. Sci., 437 (2013) 90–98.
[8] N.N. Thinh, P.T.B. Hanh, T.T.H. Le, N.A. Le, T.V. Hoang, V.D. Hoang, H.D. Le, N.V. Khoi, T.D. Lam, Magnetic chitosan nanoparticles for removal of Cr(VI) from aqueous solution, Mat. Sci. Eng. C, 33 (2013) 1214–1218.
[9] P. Thamilarasu, K. Karunakaran, Kinetic, equilibrium and thermodynamic studies on removal of Cr(VI) by activated carbon prepared from Ricinus communis seed shell, Can. J. Chem. Eng., 91 (2013) 9–18.
[10] X. Lv, J. Xu, G. Jiang, X. Xu, Removal of chromium(VI) from wastewater by nanoscale zero-valent iron particles supported on multiwalled carbon nanotubes, Chemosphere, 85 (2011) 1204–1209.
[11] L. Li, F. Zhu, Y. Lu, J. Guan, Synthesis, adsorption and selectivity of inverse emulsion Cd(II) imprinted polymers, Chinese J. Chem. Eng., in press.
[12] H.T. Fan, Y. Lu, A.J. Liu, B. Jiang, H. Shen, C. Huang, W.X. Li, A method for measurement of free cadmium species in waters using diffusive gradients in thin films technique with an ion-imprinted sorbent, Anal. Chimi. Acta, 897 (2015) 24–33.
[13] G. Bayramoglu, M. Yakup Arica, Synthesis of Cr(VI)-imprinted poly(4-vinyl pyridine-co-hydroxyethyl methacrylate) particles: Its adsorption propensity to Cr(VI), J. Hazard. Mater., 187 (2011) 213–221.
[14] V. Pakade, E. Cukrowska, J. Darkwa, N. Torto, L. Chimuka, Selective removal of chromium (VI) from sulphates and other metal anions using an ion-imprinted polymer, Water SA, 37 (2011) 529–537.
[15] A. Nastasović, Z. Sandić, Lj. Suručić, D. Maksin, D. Jakovljević, A. Onjia, Kinetics of hexavalent chromium sorption on amino-functionalized macroporous glycidyl methacrylate copolymer, J. Hazard. Mater., 271 (2009) 153–159.
[16] Q.F. An, J.B. Gao, Adsorption characteristics of Cr(III) ionic imprinting polyamine on silica gel surface, Desalination, 249 (2009) 1390–1396.
[17] F. Zhu, Y. Lu, L. Li, Synthesis, adsorption kinetics and thermodynamics of ureido-functionalized Pb(II) surface imprinted polymers for selective removal of Pb(II) in wastewater, RSC Adv., 6 (2016) 111–120.
[18] Y. Li, B. Gao, R. Du, Studies on Preparation and Recognition Characteristic of Surface-Ion Imprinting Material IIP-PEI/SiO^2 of Chromate Anion, Separ. Sci. Technol., 46 (2011) 1472–1481.
[19] Y. Liu, X. Meng, J. Han, Z. Liu, M. Meng, Y. Wang, R. Chen, S. Tian, Speciation, adsorption and determination of chromium(III) and chromium(VI) on a mesoporous surface imprinted polymer adsorbent by combining inductively coupled plasma atomic emission spectrometry and UV spectrophotometry, J. Sep. Sci., 36(2013) 3949–3957.
[20] M. Yiğitoğlu, M. Arslan, selective removal of Cr(VI) anions from aqueous solutions including Cr(VI), Cu(II) and Cd(II) ions by 4-vinly pyridine/2-hydroxyethylmethacrylate monomer mixture grafted poly(ethylene terephthalate) fiber, J. Hazard. Mater., 166 (2009) 435–444.
[21] Y. Hong, Z. Zhong, Kinetics of adsorption of Zn^{2+} on imprinted chitosan polymer, Chem. Indust. Eng. Pro., 2011 (30) 1290–1301.
[22] D.K. Singh, S. Mishra, Synthesis and characterization of Hg(II)-ion-imprinted polymer: Kinetic and isotherm studies, Desalination, 257 (2010) 177–183.
[23] Y.S. Ho, G. McKay, Pseudo-second-order model for sorption processes, Process Biochem., 34 (1999) 451–465.
[24] Y.S. Ho, J.C.Y. Ng, G. McKay, Kinetics of pollutant sorption by biosorbents: review. Sep. Purif. Methods, 29 (2000) 189–232.
[25] Z. Ren, D. Kong, K. Wang, W. Zhang, Preparation and adsorption characteristics of an imprinted polymer for selective removal of Cr(VI) ions from aqueous solutions, J. Mater. Chem. A., 2(42) (2014) 17952–17961.
[26] H.T. Fan, W. Sun, B. Jiang, Q. Wang, D. Li, C. Huang, K. Wang, Z. Zhang, W. Li, Adsorption of antimony(III) from aqueous solution by mercapto-functionalized silica-supported organic–inorganic hybrid sorbent: Mechanism insights, Chem. Eng. J., 286 (2016) 128–138.